

Portland State University

PDXScholar

Civil and Environmental Engineering Faculty
Publications and Presentations

Civil and Environmental Engineering

1-9-2023

Dissecting succulence: Crassulacean acid metabolism and hydraulic capacitance are independent adaptations in *Clusia* leaves

Alistair Leverett
Newcastle University

Samantha Hartzell
Portland State University, s.hartzell@pdx.edu

Klaus Winter
Smithsonian Tropical Research Institute, Balboa

Milton Garcia
Smithsonian Tropical Research Institute, Balboa

multiple additional authors

Follow this and additional works at: https://pdxscholar.library.pdx.edu/cengin_fac



Part of the [Civil and Environmental Engineering Commons](#)

Let us know how access to this document benefits you.

Citation Details

Leverett, A., Hartzell, S., Winter, K., Garcia, M., Aranda, J., Virgo, A., ... & Borland, A. M. (2022). Dissecting succulence: Crassulacean acid metabolism and hydraulic capacitance are independent adaptations in *Clusia* leaves. *Plant, Cell & Environment*.

This Article is brought to you for free and open access. It has been accepted for inclusion in Civil and Environmental Engineering Faculty Publications and Presentations by an authorized administrator of PDXScholar. Please contact us if we can make this document more accessible: pdxscholar@pdx.edu.

Dissecting succulence: Crassulacean acid metabolism and hydraulic capacitance are independent adaptations in *Clusia* leaves

Alistair Leverett^{1,2} | Samantha Hartzell³ | Klaus Winter² | Milton Garcia² | Jorge Aranda² | Aurelio Virgo² | Abigail Smith¹ | Paulina Focht¹ | Adam Rasmussen-Arda¹ | William G. T. Willats¹ | Daniel Cowan-Turner¹ | Anne M. Borland¹

¹School of Natural and Environmental Sciences, Newcastle University, Newcastle Upon Tyne, UK

²Smithsonian Tropical Research Institute, Balboa, Ancón, Republic of Panama

³Department of Civil and Environmental Engineering, Portland State University, Portland, Oregon, USA

Correspondence

Alistair Leverett and Anne M. Borland, School of Natural and Environmental Sciences, Newcastle University, Newcastle Upon Tyne NE1 7RU, UK.

Email: a.leverett@essex.ac.uk and anne.borland@ncl.ac.uk

Samantha Hartzell, Department of Civil and Environmental Engineering, Portland State University, 1930 SW 4th Ave, Portland, OR, USA.

Email: shartz2@pdx.edu

Funding information

Smithsonian Tropical Research Institute Short-Term Fellowship; R. B. Cook Scholarship

Abstract

Succulence is found across the world as an adaptation to water-limited niches. The fleshy organs of succulent plants develop via enlarged photosynthetic chlorenchyma and/or achlorophyllous water storage hydrenchyma cells. The precise mechanism by which anatomical traits contribute to drought tolerance is unclear, as the effect of succulence is multifaceted. Large cells are believed to provide space for nocturnal storage of malic acid fixed by crassulacean acid metabolism (CAM), whilst also buffering water potentials by elevating hydraulic capacitance (C_{FT}). The effect of CAM and elevated C_{FT} on growth and water conservation have not been compared, despite the assumption that these adaptations often occur together. We assessed the relationship between succulent anatomical adaptations, CAM, and C_{FT} , across the genus *Clusia*. We also simulated the effects of CAM and C_{FT} on growth and water conservation during drought using the Photo3 model. Within *Clusia* leaves, CAM and C_{FT} are independent traits: CAM requires large palisade chlorenchyma cells, whereas hydrenchyma tissue governs interspecific differences in C_{FT} . In addition, our model suggests that CAM supersedes C_{FT} as a means to maximise CO_2 assimilation and minimise transpiration during drought. Our study challenges the assumption that CAM and C_{FT} are mutually dependent traits within succulent leaves.

KEYWORDS

capacitance, *Clusia*, crassulacean acid metabolism, succulence

This is an open access article under the terms of the Creative Commons Attribution License, which permits use, distribution and reproduction in any medium, provided the original work is properly cited.

© 2023 The Authors. *Plant, Cell & Environment* published by John Wiley & Sons Ltd.

1 | INTRODUCTION

The advent of global warming is expected to cause more frequent and severe drought events to ecosystems, worldwide (Jiao et al., 2021; Sheffield & Wood, 2008). To prepare for increased aridity, it is imperative that scientists develop a thorough understanding of the adaptations that plants currently employ to survive drought in nature (Borland et al., 2015; Fradera-Soler et al., 2021; Germon et al., 2019; Heyduk, Grace, et al., 2021; Trueba et al., 2019; Yang et al., 2020). One adaptation that can be found across the world's semi-arid ecosystems is succulence (Arakaki et al., 2011; Jolly et al., 2020;

Merklinger et al., 2021). Succulent plants can be recognised by their fleshy leaves and/or stems, which can store substantial volumes of water long after rainfall events have ended. Despite having evolved convergently across the globe, succulence is a complex syndrome that can develop in several different ways: water can be stored within large photosynthetic chlorenchyma cells, and/or in specialised achlorophyllous water-storage hydrenchyma cells (Figure 1) (Borland et al., 2018; Heyduk, 2021; Males, 2017; Ogburn & Edwards, 2010). The consequence of succulence is multifaceted, often thought to be affecting both photosynthetic and hydraulic physiology. One key photosynthetic adaptation associated with succulence is crassulacean

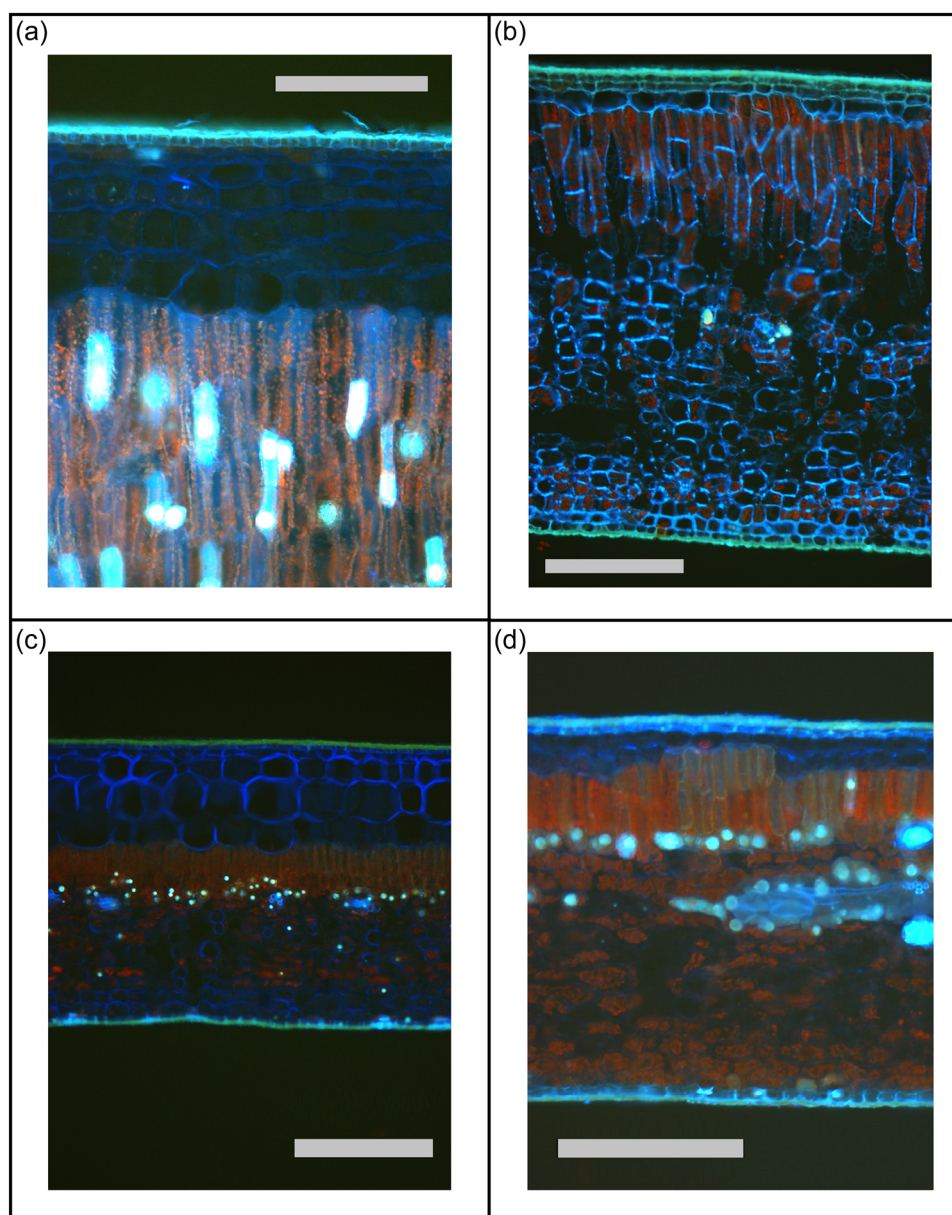


FIGURE 1 Anatomy of *Clusia* leaves, showing achlorophyllous hydrenchyma and photosynthetic chlorenchyma (comprised of palisade and spongy mesophyll layers). (a) Constitutive CAM species, *Clusia alata*, has thick hydrenchyma and thick chlorenchyma. (b) Constitutive CAM species, *Clusia rosea*, has thick chlorenchyma and shallow hydrenchyma. (c) Obligate C_3 species, *Clusia multiflora*, has thick hydrenchyma and shallow chlorenchyma (d) Obligate C_3 species, *Clusia grandiflora*, has shallow hydrenchyma and shallow chlorenchyma. For all images, scale bars represent 250 μm . [Color figure can be viewed at wileyonlinelibrary.com]

acid metabolism (CAM). In contrast to C_3 photosynthesis, CAM plants assimilate the majority of their CO_2 at night, temporarily fixing carbon into malic acid and storing it in the vacuole until the following day. By fixing CO_2 at night, rather than during the day, CAM allows stomata to open when the atmosphere is cooler and more humid, which curtails transpirational water losses (Abraham et al., 2020; Winter et al., 2005). CAM requires large succulent chlorenchyma cells to provide sufficient space to store malic acid overnight (Barrera-Zambrano et al., 2014; Males, 2018; Nelson et al., 2005; Töpfer et al., 2020; Yamaga-Hatakeyama et al., 2022). However, succulence also performs a further, hydraulic function, by elevating bulk hydraulic capacitance (C_{FT}) (Borland et al., 2018; Ogburn & Edwards, 2012). C_{FT} is defined as the ratio with which relative water content (RWC) and water potential (Ψ) drop during dehydration, multiplied by the moles of stored water in a given leaf area (Equation 2). Organs with higher C_{FT} can lose more water without severe drops to Ψ , thereby avoiding hydraulic damage to vascular and mesophyll tissues (Brodrribb et al., 2016; John et al., 2018; Scoffoni et al., 2017; Zhang et al., 2016). Therefore, succulence can help plants survive drought by aiding the CAM pathway which minimises water loss, and by elevating C_{FT} , to buffer water potentials during dehydration.

As CAM and high C_{FT} are both believed to act as adaptations to drought, it is uncertain whether one trait or both have driven the evolution of succulence. Strong CAM species often have large, tightly packed photosynthetic chlorenchyma, whereas most studies find little to no correlation between hydrenchyma thickness and CAM expression (Barrera-Zambrano et al., 2014; Males, 2018; Martin et al., 2019). However, as CAM plants are typically found in water-limited niches, it is unclear whether large chlorenchyma cells truly exist to provide vacuole space for malic acid, or if this anatomical adaptation is in fact a consequence of maximising C_{FT} to buffer plant water potentials during drought. A third possibility is that large chlorenchyma cells may have evolved to serve a dual function: providing space for malic acid storage and increasing C_{FT} (Edwards, 2019). Moreover, it is unclear if the presence of succulent hydrenchyma tissue can obviate the need for large chlorenchyma cells to provide C_{FT} . If this were the case, it would indicate that large chlorenchyma cells are not playing a dual role, but are in fact a direct consequence of the evolution of strong CAM physiology. Building a robust physiological framework to describe the relationship between anatomy and C_{FT} is required to fully understand the role that succulence plays in facilitating CAM and address the potentially confounding effect that C_{FT} has on the relationship between large chlorenchyma cells and CAM. It is also unclear how CAM and C_{FT} interact to affect plant physiology during drought (Veste & Herppich, 2021). Both characteristics are thought to buffer declines in plant Ψ during drought, but it is not known if these adaptations function synergistically or if the presence of one obviates the need for the other. In short, whilst it is often assumed that CAM and elevated C_{FT} are found together, very little has been done to disentangle the effects that these adaptations have on plant physiology during drought. The use of modelling is ideal for this

purpose, as it would allow CAM and C_{FT} to each be independently altered, whilst keeping other traits constant (Chomthong & Griffiths, 2020; Luo et al., 2021).

To disentangle the roles of CAM and C_{FT} in succulent leaves, we analysed *Clusia*, a large phenotypically diverse genus of trees and hemiepiphytes from Central and South America and the Caribbean (Borland et al., 1992; Holtum et al., 2004; Leverett et al., 2021, 2022; Luján et al., 2021; Pachon et al., 2022; Tinoco Ojanguren, & Vázquez Yanes, 1983). Under well-watered conditions, *Clusia* leaves contain a diversity of photosynthetic phenotypes, ranging from obligate C_3 , to strong CAM (Barrera-Zambrano et al., 2014). This range includes several species exhibiting C_3 -CAM intermediate phenotypes, where metabolic flux through the CAM cycle represents only a small to moderate fraction of total carbon assimilation (Tay et al., 2020; Winter, 2019). In addition, many *Clusia* species exhibit facultative CAM phenotypes, meaning they can increase metabolic flux through the CAM cycle in response to drought (Leverett et al., 2021; Winter & Holtum, 2014). Furthermore, the leaves of *Clusia* exhibit a high degree of anatomical diversity (Luján et al., 2021). Across a well characterised glasshouse collection of *Clusia*, CAM was found to correlate with enlarged palisade chlorenchyma cells (Barrera-Zambrano et al., 2014). Moreover, across this *Clusia* collection there is substantial interspecific variation in adaxial hydrenchyma cell size and tissue thickness, which is independent of CAM (Barrera-Zambrano et al., 2014; Borland et al., 2018). High photosynthetic and anatomical variation within closely related species makes it possible to conduct comparative analyses (Scoffoni et al., 2016), which we used to dissect the roles of hydrenchyma from those of large palisade chlorenchyma cells. We interrogated the same *Clusia* collection as Barrera-Zambrano et al. (2014) to determine if large chlorenchyma cells associated with CAM also result in elevated C_{FT} . Furthermore, we investigated saturated water content (SWC is $g\ water\ g^{-1}\ dry\ mass$), cell wall characteristics and osmotic properties of leaves to understand the physiological traits that lead to interspecific differences in C_{FT} . Finally, we parameterised the recently developed Photo3 model (Hartzell et al., 2018, 2021) with *Clusia* data, to establish the roles that CAM and C_{FT} each play during drought. Together, these analyses deconstruct the assumption that CAM and C_{FT} are mutually dependent traits within succulent leaves.

2 | MATERIALS AND METHODS

2.1 | Plant growth conditions

Comparative analyses were conducted on the same population of *Clusia* species that was characterised by Barrera-Zambrano et al. (2014), grown under standardised conditions. Plants in this glasshouse collection are propagated from cuttings. The species studied were: CAM species—*Clusia rosea* Jacq., *C. fluminensis* Planch. & Triana, *Clusia alata* Planch. & Triana, *C. hilariana* Schltld; C_3 -CAM species: *C. lanceolata* Cambess., *C. aripoensis* Britton and *C. minor* L.; obligate C_3 species—*Clusia multiflora* Kunth, *C. tocuchensis* Britton

and *C. grandiflora* Splitg (Supporting Information: Table S4). Plants aged 3–6 years (approx. 60–100 cm tall) were grown in 3:1, (v/v) compost-sand mixture (John Innes No. 2, Sinclair Horticulture Ltd.), in 10 L pots. 12 replicate plants were available per species, but some experiments used fewer replicates due to space limitations and/or the nature of the analysis. Plants were lit with sunlight plus photosynthetic LED lights (Attis 5 LED plant growth light, PhytoLux) to ensure that a 12 h photoperiod was maintained throughout the year. Plants were watered every 2 days and glasshouse temperatures were maintained at 25 and 23°C during the day and night, respectively.

In addition to our comparative analysis across 11 species, we conducted further experiments on two of these species after dissecting hydrenchyma tissue from abaxial chlorenchyma (described in more detail below). *C. alata* (constitutive CAM) and *C. tocuchensis* (obligate C_3) plants were used for this purpose, on the basis that, of the species studied, they showed the thickest hydrenchyma layers for constitutive CAM (*C. alata*) or obligate C_3 (*C. tocuchensis*) and were thus the species most amenable for dissection. Individuals were taken from the same population of *Clusia* plants used for comparative analyses described above. To measure diel fluctuations in RWC of the hydrenchyma tissue, plants were transferred to a growth chamber, to ensure plants were grown under stable light and temperature regimes. 3–4-year-old plants were transferred from the glasshouse collection to a plant growth chamber (SANYO Fitotron) and allowed to acclimatise for 3 weeks (12 h light period, day/night temp 25/19°C). Plants received approximately $500 \mu\text{mol m}^{-2} \text{s}^{-1}$ PFD at leaf height and were watered every 2 days.

2.2 | Gas exchange

For comparative analyses of 11 species, published gas exchange data were used as a quantitative estimate of investment in CAM (Barrera-Zambrano et al., 2014; Leverett et al., 2021). These gas exchange data were generated from the same population of plants grown under the same, standardised glasshouse conditions as those used in the present study. For gas exchange measurements, glasshouse-grown plants were temporarily moved to a controlled growth room, and left to equilibrate for 3 weeks, under well-watered conditions. At the start of each gas exchange measurement, watering was withheld, to capture photosynthetic rates as plants became droughted. At the start of each measurement, leaves were inserted into a compact mini cuvette system, Central Unit CMS-400 linked to a BINOS-100 infra-red gas analyser (HeinzWalz GmbH), and CO_2 gas exchange was recorded every 20 min for 12 days. A quantitative estimate of CAM was established by measuring the percentage of diel CO_2 assimilation occurring at night under well-watered conditions ($\text{CAM}_{\text{w/w}}$) and after 9 days of drought (CAM_{d}) (Barrera-Zambrano et al., 2014; Leverett et al., 2021).

To accompany the dissection experiments (described below) diel gas exchange traces were measured for two species, *C. alata* and *C.*

tocuchensis, under well-watered conditions. These measurements were made in a growth chamber, to ensure stable temperatures and light intensities. Stomatal conductance to H_2O , g_s ($\text{mol m}^{-2} \text{s}^{-1}$), for *C. alata* and *C. tocuchensis*, was recorded using a LI-6400XT infra-red gas analyser (LiCOR). Leaves were sealed into a leaf chamber fluorometer cuvette, set to track external light conditions with humidity maintained around 60% and data was logged every 15 min. Three biological replicates were made for each species, and one representative graph is included to show stomatal conductance for each species.

2.3 | Pressure–volume curves

Pressure–volume curve data for 11 *Clusia* species were taken from Leverett et al. (2021). These data were used to plot leaf water potential (Ψ_L) or turgor pressure (P) against RWC, where:

$$\text{RWC} = \frac{\text{leaf fresh mass} - \text{leaf dry mass}}{\text{rehydrated leaf fresh mass} - \text{leaf dry mass}}. \quad (1)$$

Bulk hydraulic capacitance, C_{FT} ($\text{mol m}^{-2} \text{MPa}^{-1}$), was calculated as:

$$C_{\text{FT}} = \frac{\delta \text{RWC}}{\delta \Psi_L} \times \text{WMA}/M_{\text{H}_2\text{O}}, \quad (2)$$

where WMA is leaf water mass per leaf area (g m^{-2}) and $M_{\text{H}_2\text{O}}$ is the molar mass of water (Beadle et al., 1985; Blackman & Brodribb, 2011; Males & Griffiths, 2018). The bulk modulus of cell wall elasticity, ϵ (MPa), was calculated as:

$$\epsilon = \frac{\delta P}{\delta \text{RWC}}. \quad (3)$$

For pressure–volume curves, $n = 6$.

2.4 | Saturated water content (SWC)

Branches were cut and moved to the lab, in bags filled with wet tissues, to minimise dehydration. The fourth leaf from the apex of each branch was cut, underwater in deionised water. Leaves were placed inside a clear bag, ensuring that cut petioles remained submerged, and sprayed with a mist of water. Leaves were left for 24 h at 25°C to fully hydrate. The following day, leaves were weighed to estimate fresh weight (FW). A 2 × 3 cm region of leaf, excluding the midrib, was cut from the leaf and used for hand-sections, to image leaf anatomy (discussed in more detail below). All leaf material, (i.e., the entire leaf including the material that was used for sectioning) was then dried at 75°C for 48 h, then weighed to estimate dry weight (DW). SWC ($\text{g H}_2\text{O g}^{-1}$ dry weight) was calculated as

$$\text{SWC} = \frac{\text{FW} - \text{DW}}{\text{DW}}. \quad (4)$$

2.5 | Anatomical measurements and statistical comparison to C_{FT}

To robustly compare anatomy with C_{FT} , two statistical approaches were employed. First, palisade, spongy mesophyll and hydrenchyma cell size data were compared to estimates of C_{FT} , derived from pressure–volume curves. For this comparison, published cell size data generated from the same *Clusia* collection, grown under the same conditions, were compared to estimates of C_{FT} (Barrera Zambrano et al., 2014; Borland et al., 2018). This approach compared species-level averages, which were analysed using linear regression models (Figure 3a–c). Second, we sought to generate leaf-level averages, with greater replication, in order to incorporate all three tissue layers into a single statistical model. To this end, we built a linear mixed effect model to estimate C_{FT} based on SWC [fixed effect] and species [random effect], as SWC has previously been shown to be a strong predictor of C_{FT} in other taxa (Ogburn & Edwards, 2012). Modelled C_{FT} correlated tightly with measurements from pressure–volume curves (Supporting Information: Figure S1: slope = 1.07, $R^2 = 0.95$, $p < 0.0001$). Using this model, C_{FT} could be estimated, alongside tissue thickness for each individual leaf. Estimates of tissue thickness were generated by hand sectioning leaf lamina, midway along the proximal–distal axis. Sectioned material was imaged using a Leitz Diaplan and a GXCAM HiChrome-S camera (GT Vision Ltd.), or a with a Leica DM6B microscope and a Leica DFC9000 sCMOS camera (Leica microsystems). These leaf-level data were used to construct linear mixed effect models to assess the relationships between tissue thickness and C_{FT} ($n = 12$). Hydrenchyma, palisade and spongy mesophyll thickness were included as fixed effects and species was used as a random effect variable. These linear mixed effect models allowed us to compare models with and without palisade thickness, using likelihood ratio tests, and hence determine whether removing palisade thickness from our model had a significant effect on the model fit. As data used for these analyses originates from both the current study and published work, a trait-by-data-source table is included in the Supporting Information: (Table S4).

2.6 | Dissection and measurement of relative water content

Hydrenchyma and chlorenchyma tissues were dissected in *C. alata* and *C. tocuchensis* since these species contain thick hydrenchyma, making them amenable to dissection (Supporting Information: Figure S2). Hydrenchyma tissue was removed from chlorenchyma, using the blunt edge of a razor. Dissected material was inspected, using a Leica DM6B microscope (Supporting Information: Figure S3) to ensure that clean separation was possible. Each dissection took < 1 s. Dissected material for *C. alata* and *C. tocuchensis* was used to assess dynamic changes in RWC over 24 h and for Comprehensive Microarray Polymer Profiling (CoMPP).

RWC was measured every 4 h for 24 h by quickly weighing dissected material which was then placed in deionised water to

rehydrate for 8 h. Chlorenchyma tissue often sank, indicating that internal air space was filling with water and altering the validity of these data (Arndt et al., 2015). Consequently, only the RWC of the hydrenchyma could be analysed and was calculated according to Equation 1.

2.7 | Structural carbohydrate profiling

Comprehensive Microarray Polymer Profiling (CoMPP) was performed according to the methodology of Moller et al., (2007), with slight adjustments. Tissue was ground with pestle and mortar in liquid nitrogen, then mixed with 70 % ethanol (1 ml). Samples were centrifuged (12 000g, 10 min) and the supernatant discarded. This was repeated with methanol:chloroform (1:1 ratio, 1 ml), followed by acetone, and pellets were left to dry overnight to form an alcohol insoluble residue (AIR).

Cyclohexanediaminetetraacetic acid (CDTA) and NaOH were used to sequentially extract polysaccharides from AIR samples. A noncontact microarray printer (Arrayjet) was used to print samples onto a nitrocellulose membrane, and these arrays were probed (each array probed separately) with a panel of antibodies with specificities for different polysaccharide epitopes. Relative spot signal intensities arising from antibody binding were determined using microarray analysis software (ArrayPro-Analyser; Media Cybernetics) before creating a heatmap based on mean signal intensities.

2.8 | Titratable acidity and osmometry

Leaves were harvested 15 min before dawn and before dusk for *C. alata* and *C. tocuchensis*. A 2–3 cm² rectangle of leaf lamina was cut midway along the proximal–distal axis of the leaf. The hydrenchyma and chlorenchyma layers were dissected, and these tissue layers were immediately frozen in liquid nitrogen. Frozen samples were crushed using a tissue lyser (Quiagen), incubated in 80 % methanol (Fisher) for 45 min and centrifuged at 14000g for 10 min. The supernatant was titrated against 0.5 Mol NaOH (Sigma), using phenolphthalein (Sigma) as an indicator, to determine H⁺ concentration.

Osmolality was measured for the same dawn–dusk samples using an Osmomat 030 cryoscopic osmometer (Gonotec). Lysed leaf tissue was vortexed in 200 μ l deionised water, and 20 μ l of this extract was placed into the osmometer to determine osmolality (Osmol kg⁻¹). The osmotic potential was calculated according to the van't Hoff equation.

2.9 | Statistics

Statistics were performed with R, v.3.6.0. Linear mixed effect models were built with the package “nlme.”

Pressure–volume curve parameters that are absolute (i.e., units are expressed on a per leaf area basis) were compared with absolute

anatomical estimates, such as tissue thickness or cell size. Pressure–volume curve parameters that are relative were compared with relative anatomical estimates, that is, percentage of leaf thickness comprised of hydrenchyma.

The source of all data used in this study is included in Supporting Information: Table S4.

2.10 | Modelling of CAM and hydraulic capacitance

The previously developed Photo3 model, which uses recent advances in CAM modelling (Bartlett et al., 2014; Hartzell et al., 2015) to represent both C_3 and CAM photosynthesis (Hartzell et al., 2018) was parameterised with published photosynthetic traits from *Clusia*. In addition, the model was parameterised with the maximum and minimum C_{FT} values recorded in this study (*C. alata* and *C. grandiflora*, respectively), plus additional data collected for this purpose (Supporting Information: File 1). The model was run using climatic data from Gamboa, Panama to simulate both static soil moisture drought and dry-down conditions (Supporting Information: File 1). Climatic data from Gamboa was used because many species of *Clusia* grow in this location.

3 | RESULTS

3.1 | Crassulacean acid metabolism (CAM) and bulk hydraulic capacitance (C_{FT}) are independent in *Clusia*

The leaves of *Clusia* are comprised of photosynthetic palisade and spongy mesophyll layers (collectively the chlorenchyma) and achlorophyllous hydrenchyma (Figure 1). Hydrenchyma cell size/tissue thickness varied independently of palisade and spongy mesophyll cell size/tissue depth (Supporting Information: Figure S4), hence the relative contribution of each tissue layer to CAM and C_{FT} could be assessed. Quantitative estimates of CAM expression used in this study were taken from Barrera-Zambrano et al. (2014) and Leverett et al. (2021), who calculated the percentage of diel net CO_2 assimilation occurring at night, in well-watered conditions and following 9 days of drought (CAM_{ww} and CAM_d , respectively; Supporting Information: Table S4). Leaf water mass per area (WMA) correlated with both CAM_{ww} and CAM_d , across 11 *Clusia* species (Figure 2a,b). However, despite containing more water, the leaves of CAM species did not exhibit elevated C_{FT} : neither CAM_{ww} nor CAM_d correlated with C_{FT} (Figure 2c,d). To understand why CAM and C_{FT} were independent, we tested the relationship between anatomical traits and C_{FT} . Linear regression analyses found relationships between species-mean estimates of hydrenchyma cell size and C_{FT} , but no such trend was observed for the cell sizes of other tissue layers (Figure 3a–c). A similar conclusion was also drawn when tissue thickness was analysed, in the place of cell size (Figure 3d–f). A linear mixed effect model found that hydrenchyma thickness significantly correlated with

C_{FT} , whereas the thickness of palisade or spongy mesophyll did not. When this model was refined to remove spongy mesophyll, the conclusion did not change: the hydrenchyma thickness significantly correlated with C_{FT} but palisade thickness did not. Additionally, palisade tissue thickness was removed from the model and the simplified model was compared to the original, using a likelihood ratio test. Removing palisade tissue thickness had no significant effect on the fit of the data, suggesting that palisade thickness did not contribute to interspecific variation in C_{FT} . Taken together, these data show that hydrenchyma, and not the palisade or spongy mesophyll, contributes to intraspecific variation in C_{FT} , in *Clusia* leaves.

We explored the relationship between CAM and SWC, as the latter has been shown to be predictive of capacitance in succulent taxa (Ogburn & Edwards, 2012). SWC did not correlate with either CAM_{ww} or CAM_d (Figure 4a,b) (linear regression: $p = 0.54$ and 0.21 , respectively). Furthermore, SWC did not correlate with leaf thickness or WMA, when data from all 11 *Clusia* species were considered together (Figure 4c,d). However, there was a clear linear relationship between WMA and SWC when only comparing species with C_3 or C_3 -CAM photosynthetic physiologies (dashed lines, Figure 4c,d). Likewise, a linear relationship existed between the WMA and SWC values for the strong CAM species (solid line, Figure 4c,d). The lack of a significant relationship between SWC and WMA in the total data set was the result of the strong CAM species having higher WMA without a corresponding higher SWC (i.e., the gap between dashed and solid lines, Figure 4c,d). This occurred because strong CAM species had higher leaf dry mass per area (LMA) (Figure 4e). Taken together, these data show that higher WMA causes leaves to have higher SWC, unless this high WMA is associated with the presence of a strong CAM phenotype. Put differently, leaves of strong CAM species have more water, but do not exhibit high SWC; the physiological characteristic typically associated with high capacitance (Ogburn & Edwards, 2012).

3.2 | Elastic cell walls confer C_{FT} in the hydrenchyma

We sought to identify the properties of the hydrenchyma that confer increased C_{FT} . One trait thought to contribute to C_{FT} is cell wall elasticity, as it allows cells to readily deform and mobilise water stores (Fradera-Soler, Grace, et al., 2022). We estimated the bulk modulus of cell wall elasticity (ϵ : a larger value represents cell walls that are highly rigid). Across 11 species of *Clusia*, C_{FT} was negatively correlated with ϵ , which in turn was negatively correlated with the percentage of leaf thickness made up of hydrenchyma (Figure 5a,b). Taken together, these data suggest that hydrenchyma cell walls are highly elastic and that this elasticity contributes to elevating C_{FT} .

To examine how the composition of hydrenchyma cell walls impacts ϵ , the structural carbohydrate composition of cell walls was analysed. Hydrenchyma was dissected from chlorenchyma in both *C. tocuchensis* (obligate C_3) and *C. alata* (constitutive CAM), and cell wall composition assessed using antibodies raised against 10 common

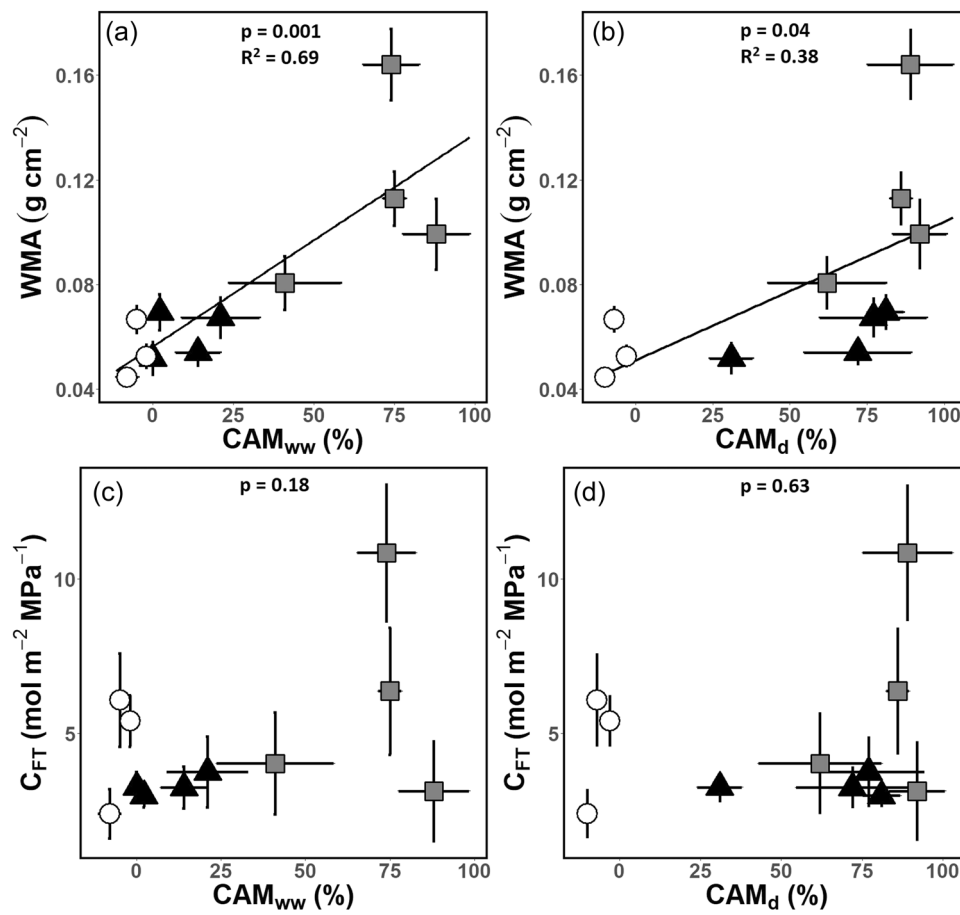


FIGURE 2 Species with Crassulacean acid metabolism have more water in leaves, but do not have elevated bulk hydraulic capacitance (C_{FT}), in *Clusia*. Quantitative estimates of CAM expression were calculated as the percentage of diel CO_2 assimilation occurring at night, in well-watered conditions and following 9 days of drought (CAM_{ww} and CAM_d , respectively). (a) Across 11 species of *Clusia*, CAM_{ww} correlated with water mass per area (WMA) (b) CAM_d also correlated with WMA. (c) CAM_{ww} did not correlate with C_{FT} . (d) CAM_d did not correlate with C_{FT} . White circles = obligate C_3 species, black triangles = C_3 -CAM intermediate species and grey squares = constitutive CAM species. For each species, $n = 6$, error bars represent ± 1 standard deviation.

polysaccharide and glycoprotein motifs. In both species, hemicelluloses (xylan, mannan and xyloglucan epitopes) were considerably less abundant in the hydrenchyma, compared with the chlorenchyma (Figure 5c–l). Together, these data suggest that low ϵ in the hydrenchyma is likely the result of this tissue having reduced structural reinforcement from hemicelluloses. In addition, in *C. alata* pectins were more abundant in the hydrenchyma than the chlorenchyma, although this pattern was not observed in *C. tocuchensis* (Supporting Information: Figure S6).

3.3 | High osmotic potentials confer C_{FT} in the hydrenchyma

Whilst low ϵ values allow hydrenchyma cells to deform to mobilise water, movement of water into the chlorenchyma can only occur if an osmotic gradient exists between the tissues. We measured the osmotic potential (π) of dissected hydrenchyma and chlorenchyma tissues in *C. alata* and *C. tocuchensis*. Values of π were higher (less

negative) in the hydrenchyma than the chlorenchyma for both species (Figure 6). In the constitutive CAM species, *C. alata*, there was a significant change in chlorenchyma π between dawn and dusk, due to fluctuations in acid content in this tissue (Figure 6a). However, π remained higher in the hydrenchyma than the chlorenchyma at both dawn and dusk (Figure 6b). In the obligate C_3 species, *C. tocuchensis*, chlorenchyma π did not differ with time. As with *C. alata*, π was higher in the hydrenchyma than the chlorenchyma at both dawn and dusk (Figure 6). Together, these data show that an osmotic gradient exists between the hydrenchyma and the chlorenchyma. In addition, these data show that fluctuations in acid contents from CAM do not eliminate this osmotic gradient.

3.4 | Diel changes to hydrenchyma relative water content

We hypothesised that elevated ϵ would allow hydrenchyma to readily inflate and deflate, to match the hydraulic needs of the leaf. Over a

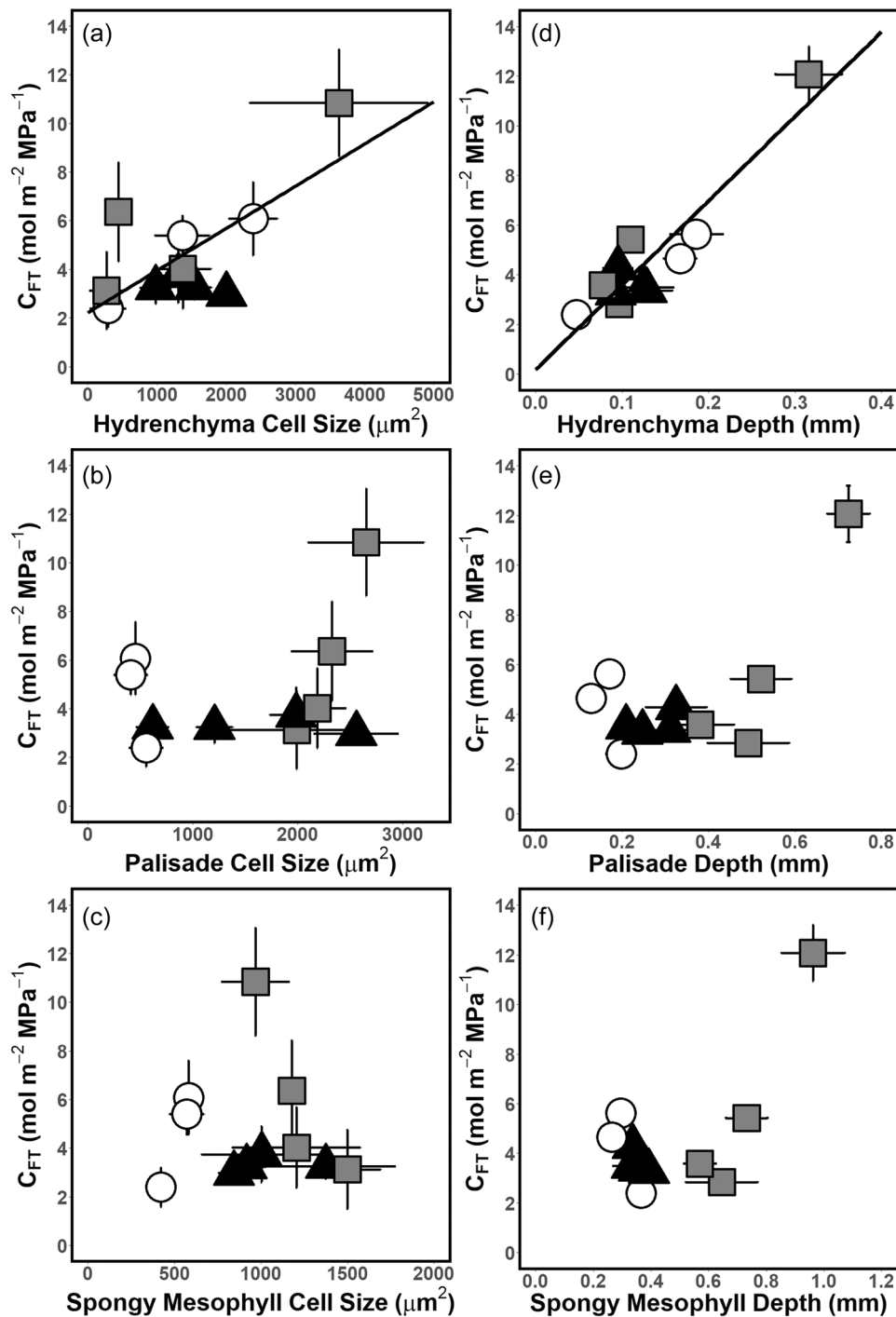


FIGURE 3 Hydrenchyma, and not the palisade or spongy mesophyll is responsible for interspecific variation in bulk hydraulic capacitance (C_{FT}). (a) Hydrenchyma cell size positively correlated with C_{FT} (linear regression: $R^2 = 0.51$; $p = 0.01$). Neither (b) palisade, nor (c) and spongy mesophyll cell size correlated with C_{FT} (linear regression: $p = 0.37$ and $p = 0.85$, respectively). (d–f) A linear mixed effect model was built to describe the relationship between tissue thickness and C_{FT} . This model found (d) a significant linear relationship between hydrenchyma thickness and C_{FT} ($p = 0.002$) but no such relationship between (e) palisade thickness and C_{FT} ($p = 0.33$) or (f) spongy mesophyll thickness and C_{FT} ($p = 0.93$). Refining this model, by removing spongy mesophyll and palisade thickness as fixed terms, had no effect on the model fit (likelihood ratio = 3.27, $p = 0.66$ when removing spongy mesophyll thickness and likelihood ratio = 3.00, $p = 0.56$ when removing palisade thickness). Note that differences in C_{FT} between graphs (a–c) and graphs (d–f) are due to the former being derived from pressure volume curves, and the latter being modelled estimates of C_{FT} . White circles = obligate C_3 species, black triangles = C_3 -CAM intermediate species and grey squares = constitutive CAM species. Error bars represent ± 1 standard deviation.

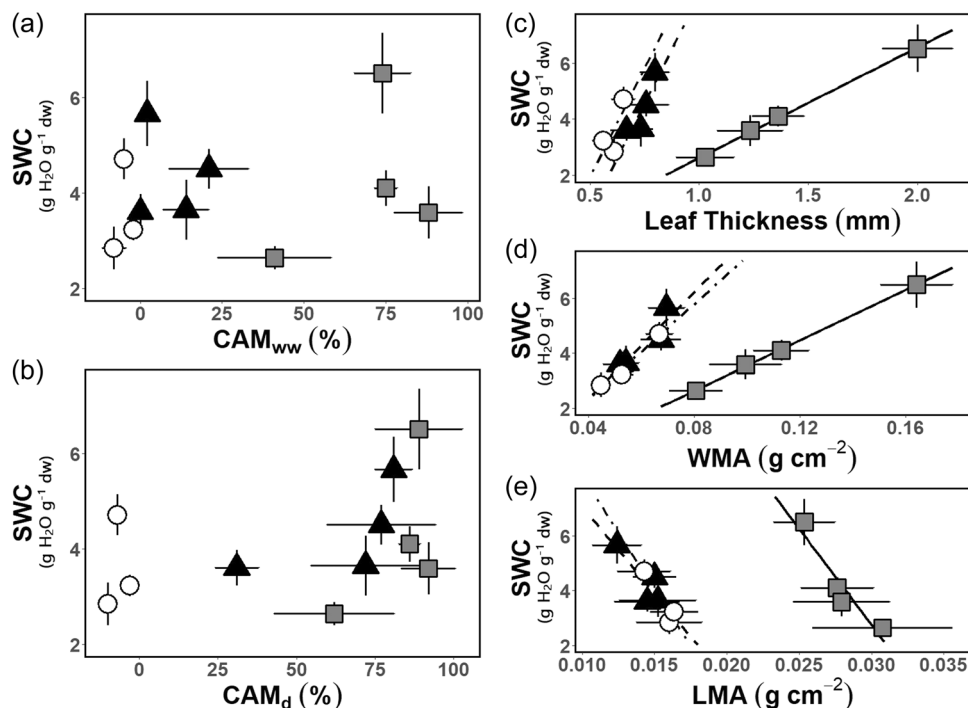


FIGURE 4 Crassulacean acid metabolism (CAM) and saturated water content (SWC) are independent in *Clusia* leaves. (a–b) Across 11 species of *Clusia*, CAM_{ww} and CAM_d did not correlate with SWC (linear regression: $p = 0.54$ and 0.21 , respectively). (c) Across 11 species of *Clusia* leaf thickness, did not correlate with SWC. However, linear relationships existed when leaf thickness was compared to SWC across species with the same photosynthetic phenotype: that is, when data from the obligate C_3 species (dot-dashed line), the C_3 -CAM species (dashed line) or the constitutive CAM species (solid line) were considered alone. (d–e) A similar trend was observed when water mass per area (WMA) or leaf dry mass per area (LMA) were compared to SWC: no correlation was found across 11 species of *Clusia*, but clear linear relationships exist when only considering species with the same photosynthetic phenotype. For all graphs, $n = 12$, white circles = obligate C_3 species, black triangles = C_3 -CAM intermediate species and grey squares = constitutive CAM species. Error bars represent ± 1 standard deviation.

24 h period, the RWC in the hydrenchyma mirrored the stomatal conductance for well-watered *C. tocuchensis* (C_3) and *C. alata* (CAM) (Supporting Information: Figure S8). When stomatal conductance was highest (during the day for *C. tocuchensis* and at night for *C. alata*), the RWC of the hydrenchyma dropped by approximately 10%. During periods of stomatal closure, the RWC of the hydrenchyma was restored to 100% (Supporting Information: Figure S8).

3.5 | CAM is more effective than C_{FT} at buffering leaf water potential during water-deficit stress

To disentangle the roles that CAM and C_{FT} play during drought, the Photo3 model was parameterised using physiological data included here for *Clusia*. The model allowed us to alter CAM and C_{FT} independently, and hence to assess their relative contributions to plant performance during a dry-down simulation. Four scenarios were simulated: high capacitance (HC) and low capacitance (LC) values in both a C_3 and a CAM leaf (HC- C_3 , LC- C_3 , HC-CAM and LC-CAM, respectively). We investigated the model responses over the course of a diel period beginning 11 days after the cessation of rain (Figure 7). Both C_3 simulations exhibited elevated net diel photosynthetic assimilation (A_n) and transpiration (E), in

comparison to the CAM simulations (Figure 7). For all simulations, the minimum daily water potential (Ψ_{min}) occurred during the day. Furthermore, both CAM simulations experienced higher (less negative) Ψ_L , which remained stable over the 24 h diel cycle unlike the C_3 simulations.

Over a 24 h period, there was a clear difference in E and A_n between the HC- C_3 and LC- C_3 simulations; for C_3 plants, elevated C_{FT} allowed stomatal conductance (g_s) to remain higher for longer, during the day. In contrast, changing C_{FT} had no discernible impact in the CAM simulations. Therefore, the presence of CAM precluded any impact of C_{FT} on diel gas exchange. A similar pattern was observed when diel Ψ_L was analysed. The HC- C_3 simulation showed substantially less diel fluctuation in Ψ_L than the LC- C_3 simulation. However, diel patterns of Ψ_L were almost identical in the HC-CAM and LC-CAM simulations. When considering the simulation of a dry season drought event, elevated C_{FT} resulted in a higher (less negative) Ψ_{min} value in both C_3 and CAM simulations. However, this only translated to a difference in cumulative E in the C_3 background: cumulative E was higher in the HC- C_3 than the LC- C_3 simulation but was not substantially different between HC-CAM and LC-CAM. C_{FT} had very little impact on A_n or WUE (besides affecting WUE when stomata were starting to shut, and gas exchange was very low). Together, these data demonstrate that the gas exchange profile of

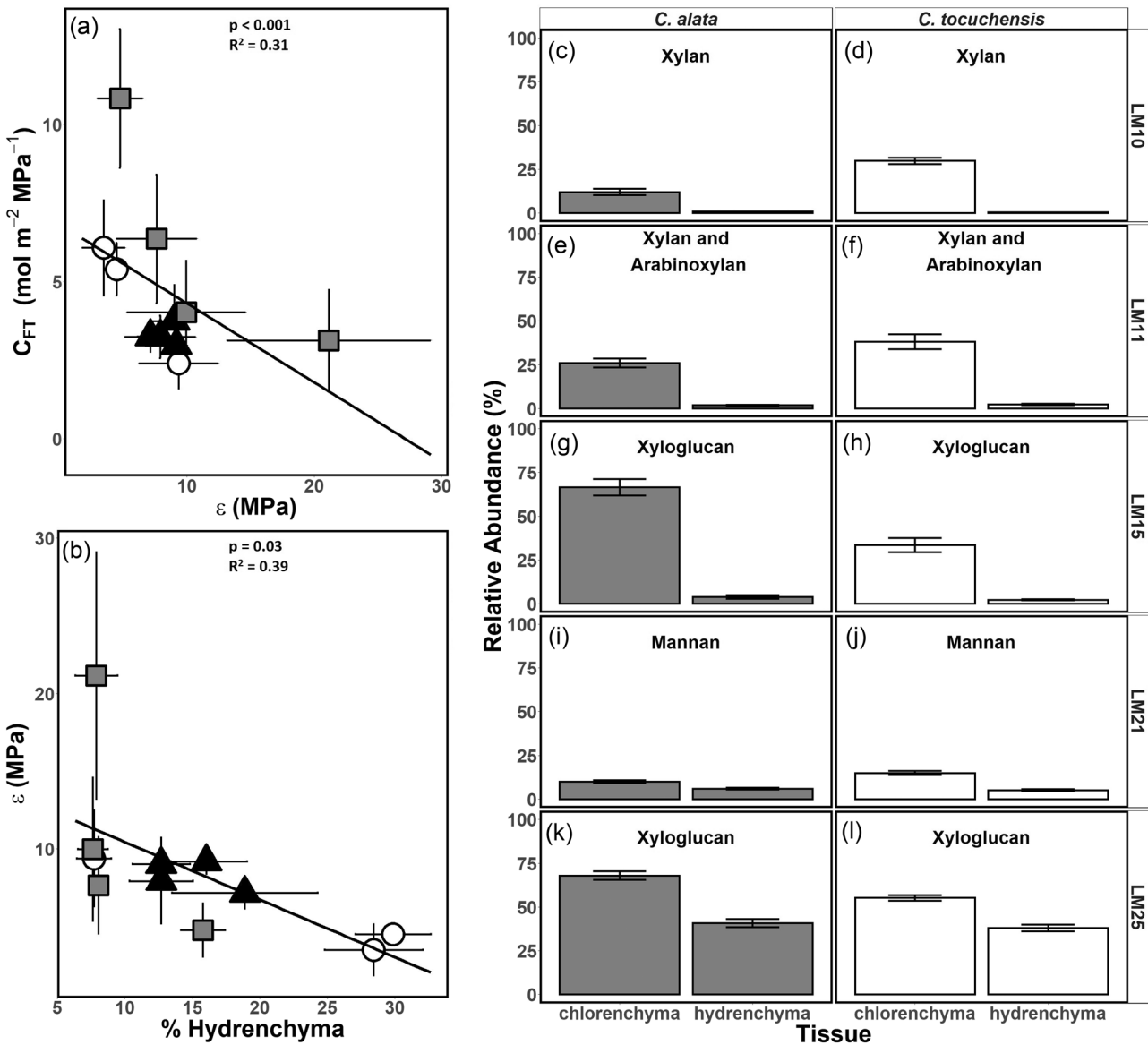


FIGURE 5 Elastic cell walls in the hydrenchyma confer elevated bulk hydraulic capacitance (C_{FT}), in *Clusia*. (a) Across 11 species of *Clusia*, the bulk modulus of cell wall elasticity (ϵ) negatively correlated with C_{FT} . (b) Across 11 species of *Clusia*, ϵ negatively correlated with the percentage of leaf thickness comprised of hydrenchyma (% hydrenchyma). (c–l) Hemicellulose contents were lower in the hydrenchyma than the chlorenchyma for both *C. alata* (constitutive CAM) and *C. tocuchensis* (obligate C_3). For graphs (c–l), p -values were < 0.001 (two tailed t -test) and conclusions were unchanged when a Bonferroni–Hochberg adjustment was applied. For graphs (a, b), $n = 6$, white circles = obligate C_3 species, black triangles = C_3 -CAM intermediate species and grey squares = constitutive CAM species, and error bars represent ± 1 standard deviation. For graphs (c–l), $n = 4$ and error bars represent ± 1 standard deviation.

CAM plants is more effective than C_{FT} at both minimising E and buffering Ψ_L .

3.6 | CAM obviates the effect of C_{FT} during prolonged drought

In addition to investigating the effect of CAM and C_{FT} over a 24 h period, the Photo3 model was used to simulate a dry-down based on climatic data from Gamboa, Panama (Figure 8), where *Clusia* plants

are known to grow. Both CAM simulations experienced lower cumulative E than the C_3 simulations. In the C_3 simulations only, higher C_{FT} caused a small increase in cumulative E after 15 days. This supports the hypothesis that CAM is more effective than C_{FT} at mitigating transpiration losses over the dry season. Furthermore, throughout the dry-down simulation, Ψ_{min} was higher (less negative) in both CAM simulations, than in either C_3 simulation. C_{FT} also caused a reduction in Ψ_{min} throughout the dry-down simulation for both photosynthetic types. However, CAM was substantially more effective than C_{FT} in mitigating drops in Ψ_{min} . These dynamics had a

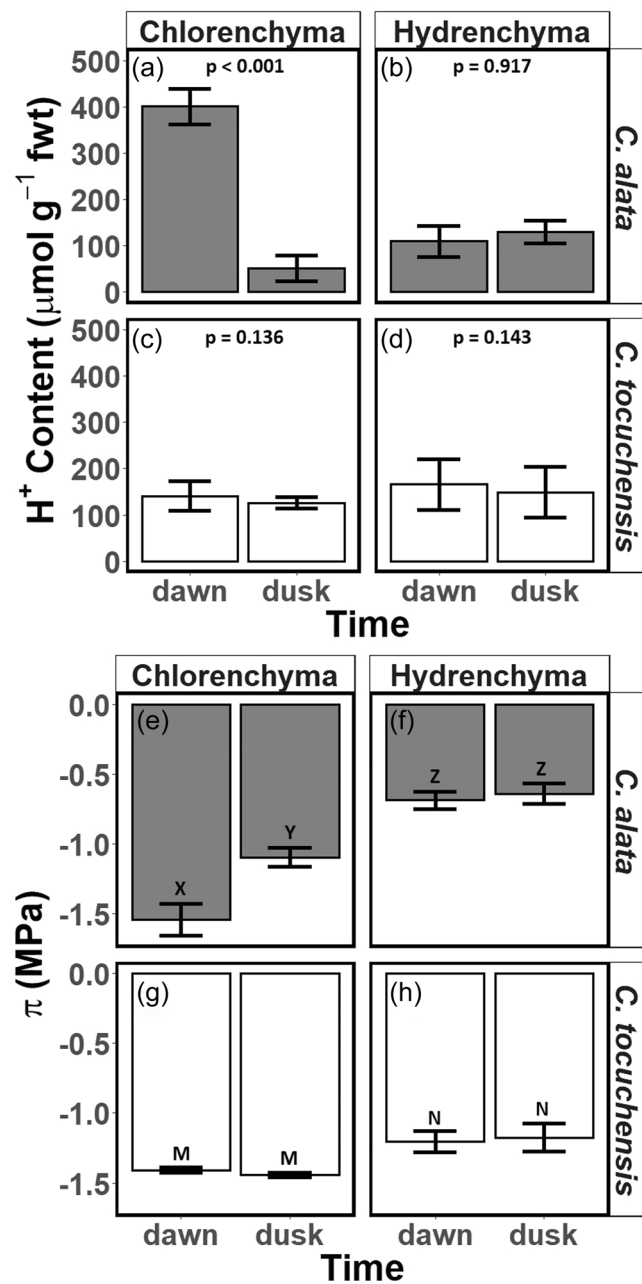


FIGURE 6 An osmotic gradient exists between hydrenchyma and chlorenchyma in *Clusia* leaves regardless of photosynthetic physiotype. (a–d) p -values come from one-tailed t -tests, comparing H⁺ contents in chlorenchyma and hydrenchyma tissues, for *C. alata* (CAM) and *C. tocuchensis* (C₃). (e–f) In *C. alata*, osmotic potential (π) differs significantly between dawn and dusk in the chlorenchyma but does not differ in the hydrenchyma. In addition, π differs significantly between chlorenchyma and hydrenchyma tissues. Letters X, Y and Z represent groupings from an ANOVA + Tukey-Kramer analysis. (g–h) In *C. tocuchensis*, π did not differ significantly between dawn and dusk in either chlorenchyma or hydrenchyma. π did differ significantly between chlorenchyma and hydrenchyma. Letters M and N represent groupings from an ANOVA + Tukey-Kramer analysis. For all graphs, $n = 4$ and error bars represent ± 1 standard deviation. ANOVA, analysis of variance.

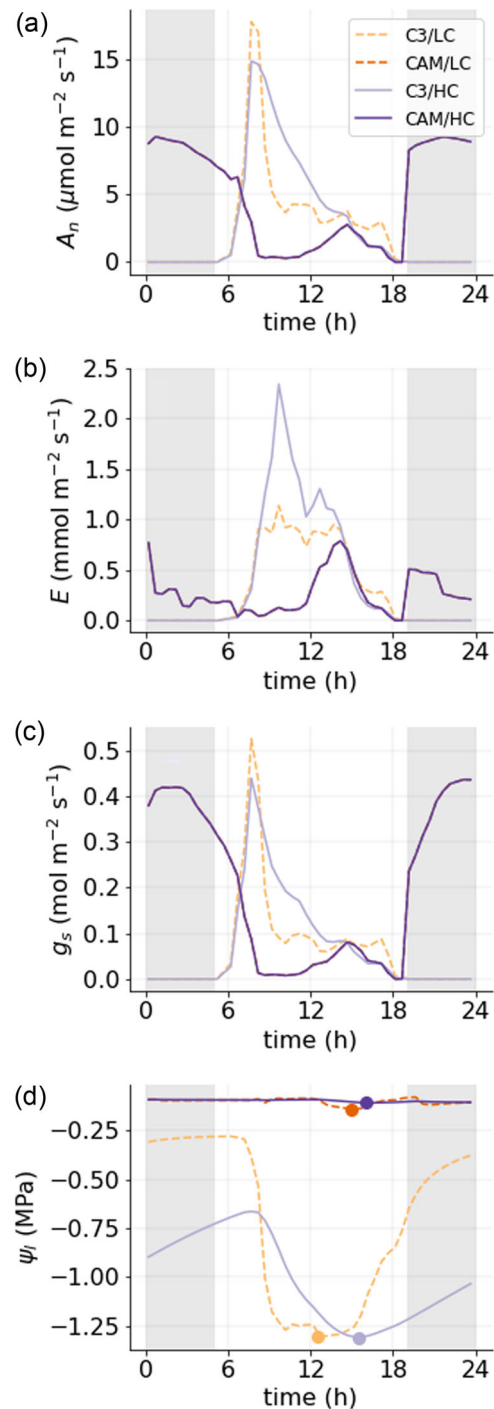


FIGURE 7 Crassulacean acid metabolism (CAM) is a more effective adaptation against drought-stress than bulk hydraulic capacitance (C_{FT}) in *Clusia* leaves. All graphs show simulated diel plant physiology, estimated using the Photo3 model after 11 days of a Panamanian dry season. (a) Diel net CO₂ assimilation (A_n). (b) Diel transpiration (E). (c) Diel stomatal exchange of H₂O (g_s). (d) Diel leaf water potential (ψ_L). [Color figure can be viewed at wileyonlinelibrary.com]

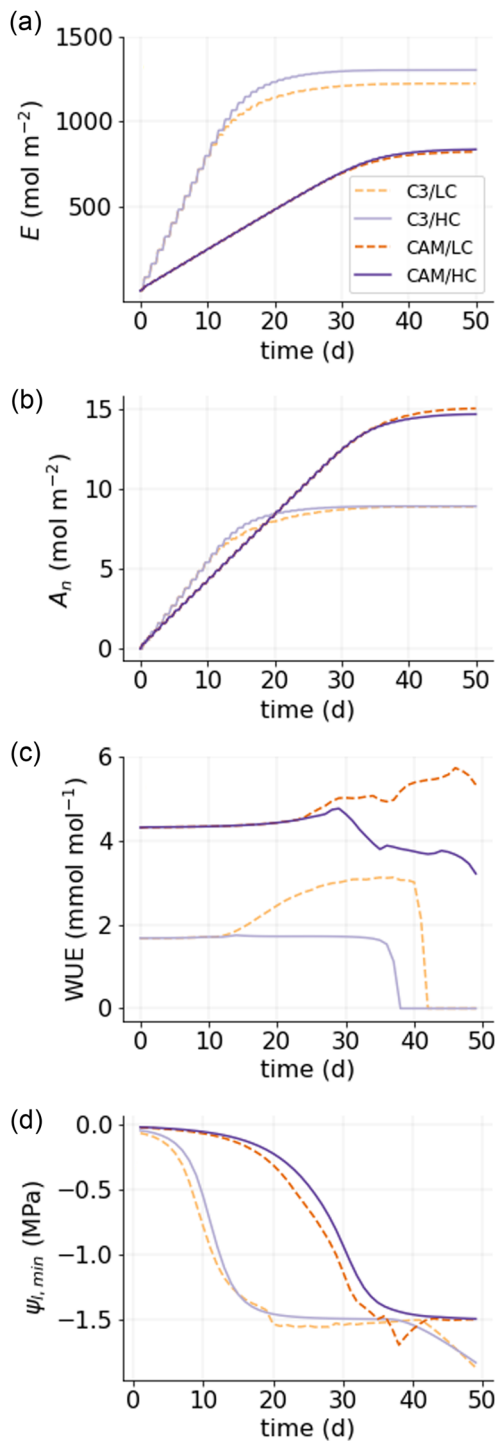


FIGURE 8 Leaf physiological traits simulated over a Panamanian dry season (a) Cumulative transpiration (E); (b) Cumulative photosynthetic assimilation (A_n); (c) Daily water use efficiency (WUE); (d) Daily minimum leaf water potential (Ψ_{min}). [Color figure can be viewed at [wileyonlinelibrary.com](https://onlinelibrary.wiley.com)]

clear impact on A_n . At the beginning of the dry-down, A_n was higher in both the C_3 scenarios than in either CAM scenario. However, approximately 18 days into the dry-down, cumulative A_n began to plateau in both C_3 scenarios. In contrast, both CAM simulations

maintained photosynthetic assimilation for 38 days. Consequently, by the end of the dry-down, both CAM scenarios had assimilated 65 % more carbon than either C_3 scenario. In contrast, C_{FT} had very little effect on A_n . Therefore, CAM was also more impactful than C_{FT} at maintaining net photosynthetic assimilation during drought. Due to higher A_n and lower E rates, both CAM scenarios exhibited higher WUE than either C_3 scenario. In contrast, C_{FT} had little effect on WUE. In summary, CAM was substantially more effective than C_{FT} at reducing E and the rate of decline in Ψ_L . Furthermore, CAM outperformed elevated C_{FT} as a means to increase net CO_2 assimilation and WUE, during the drought simulation. Taken together, these analyses indicate that the presence of CAM in *Clusia* largely obviates the effect of C_{FT} over 24 h and over the course of a dry season, as neither carbon gain nor water use was substantially affected by changes to C_{FT} in CAM simulations.

4 | DISCUSSION

4.1 | Large palisade chlorenchyma cells are an adaptation for CAM, not C_{FT} , in *Clusia*

Previous work on this *Clusia* collection has shown that palisade cell size and thickness positively correlates with CAM photosynthesis (Barrera-Zambrano et al., 2014; Borland et al., 2018). This finding is congruous with observations in other taxa, where chlorenchyma cell size is greater in CAM species than C_3 relatives (Heyduk et al., 2016; Males, 2018). However, conclusions based on correlations between anatomical adaptations and CAM suffer from the potentially confounding effect of C_{FT} . Moreover, it has been unclear if large chlorenchyma cells are in fact a requirement of CAM or whether they are instead acting to increase C_{FT} to hydraulically buffer the leaf, as this could also act as an adaptation to drought (Edwards, 2019). In *Clusia*, we found that both CAM and chlorenchyma cell sizes were independent of C_{FT} (Figures 2,3). For example, the leaves of *C. multiflora* (obligate C_3) had C_{FT} values approximately twice that of *C. hilariana* (constitutive CAM), despite leaf thickness, palisade thickness and palisade cell size being approximately 2, 3 and 4.5 times lower, respectively, in the C_3 species. *C. multiflora* had higher values of C_{FT} due to its investment in hydrenchyma, which had a twofold higher tissue thickness than in *C. hilariana*. A similar relationship between hydrenchyma and C_{FT} is also present in *Tillandsia ionantha* (Bromeliaceae), *Pyrrisia lingua* (Polypodiaceae) and *Cheilanthes myriophylla* (Pteridaceae); in which hydrenchyma tissue thickness substantially buffers leaf water potentials during drought (Mcadam & Brodribb, 2013; Nowak & Martin, 1997). In *Clusia*, across all 11 species studied, we found that the hydrenchyma, and not the chlorenchyma was responsible for interspecific differences in C_{FT} (Figure 3). Therefore, these analyses indicate that large palisade cells, in thick CAM leaves, are not acting to elevate C_{FT} , as hydrenchyma performs this function instead. By accounting for the potentially confounding effect of C_{FT} , we have increased the confidence that the correlation between palisade cell size and CAM is physiologically

meaningful within the genus *Clusia* (Barrera-Zambrano et al., 2014). Thus, this finding provides a robust demonstration that large chlorenchyma cells exist to directly aid in the storage of malic acid in the CAM cycle, rather than to hydraulically buffer Ψ_L . This physiological framework (chlorenchyma performing CAM and hydrenchyma conferring C_{FT}) provides a platform for investigations into the evolution of succulence in *Clusia*. $^{13}C/^{12}C$ isotope ratios, and hydrenchyma thickness can be used as high-throughput proxies for CAM and C_{FT} , respectively (Leverett et al., 2021; Messerschmid et al., 2021). These traits could be mapped, together, onto the recently developed phylogeny of *Clusia* to understand the eco-evolutionary dynamics that have led to leaf succulence in this genus (Luján et al., 2021).

We sought to understand why CAM species do not exhibit elevated C_{FT} , despite having thicker leaves and more water (Figure 4). Constitutive CAM species had greater WMA (Figures 2 and 4), but these species did not exhibit elevated SWC, due to their higher LMA (Figure 4). There are two possible explanations for this observation. The first is that thicker leaves are the consequence of a greater number of identical cell layers, thus elevating WMA and LMA proportionally, which would result in no change to SWC. However, this is unlikely because it is already known that CAM is associated with larger palisade cells, not more layers of identical cells, in *Clusia* (Barrera-Zambrano et al., 2014; Borland et al., 2018). This increases the likelihood of the second explanation: that constitutive CAM species have larger cells, whilst also investing more carbon in cell wall thickness and reinforcement. Such a scenario would cause CAM species to have elevated LMA, with no changes to SWC, despite having larger palisade cells with higher WMA values. Similar findings are observed in the genus *Crassula*, where larger chlorenchyma cells in thicker leaves do not amount to elevated SWC (Fradera-Soler et al., 2021). This also provides a putative explanation for why the development of thick leaves in CAM species does not increase C_{FT} . If large palisade cells in CAM species have thicker cell walls, they would become more rigid, which would in turn decrease C_{FT} , as cell wall deformations to mobilise water would occur less readily. Chlorenchyma cell wall thickness is high in a number of CAM species, such as *Agave deserti* and *Kalanchoe daigremontiana* (Maxwell et al., 1997; Smith et al., 1987). Direct analysis of cell wall thickness was outside of the scope of this study, but future work should investigate the relationship between CAM and cell wall dimensions in *Clusia* and other taxa.

4.2 | Biomechanics and osmotic properties of hydrenchyma elevate C_{FT}

Having established that the hydrenchyma, and not the chlorenchyma, is responsible for interspecific variation in C_{FT} , we sought to develop a deeper mechanistic understanding of how C_{FT} is controlled in *Clusia* leaves. Across all 11 species studied, measurements of ϵ strongly suggest that hydrenchyma cell walls are highly elastic, and that this is responsible for their contribution to C_{FT} . In addition, hemicelluloses,

which are known to provide structural reinforcement to cell walls (Kim et al., 2020; Panter et al., 2020; Vanzin et al., 2002), were found at significantly lower abundances in the hydrenchyma in comparison to the chlorenchyma (Figure 5). This finding is congruent with a recent demonstration that hemicelluloses are less abundant in the leaves of phylogenetically diverse succulent species, compared to non-succulent plants (Fradera-Soler, Leverett, et al., 2022). Furthermore, pectins, which provide flexibility and can increase water holding capacity of the apoplast, were more abundant in the hydrenchyma than the chlorenchyma in *C. alata* (Supporting Information: Figure S6) (Ahl et al., 2019; Braybrook et al., 2012; Fradera-Soler, Grace, et al., 2022; Goycoolea & Cárdenas, 2003; Sáenz et al., 2004). Together, these findings support the hypothesis that elastic cell walls are contributing to the elevated C_{FT} provided by the hydrenchyma. Elasticity allows cells to contort and mobilise water to meet the needs of the leaf. Cell walls are known to deform and fold in regular patterns in the hydrenchyma of *Pyrrosia* and *Aloe* and in the cortex of cacti, in order to release stored water during drought (Ahl et al., 2019; Mauseth, 1995; Ong et al., 1992). This allows hydrenchyma tissue to shrink as the leaf dehydrates (Supporting Information: Figure S8), thereby mitigating water loss from the chlorenchyma and maintaining Ψ_L at stable levels (Nowak & Martin, 1997).

Whilst elasticity allows cell walls to bend, the movement of water will not occur without an osmotic gradient between tissues. We found that both *C. alata* (constitutive CAM) and *C. tocuchensis* (obligate C_3) maintained an osmotic gradient between the hydrenchyma and chlorenchyma (Figure 6). Importantly, diel differences in chlorenchyma π , caused by CAM-related acid accumulation/depletion did not eradicate this osmotic gradient, meaning water can favourably move out of the hydrenchyma at all times of the day (Figure 6). A similar within-leaf osmotic gradient occurs in *Agave*, and is integral to providing C_{FT} (Schulte and Nobel, 1989; Smith et al., 1987). Together, highly elastic cell walls in conjunction with an osmotic gradient mean that interspecific variation in hydrenchyma thickness confers more than fourfold variation in C_{FT} , despite this tissue comprising only 7.5%–30% of total leaf thickness.

4.3 | CAM and C_{FT} affect growth and water loss differently during drought: Ecological implications

With the advent of global warming, succulent species are becoming increasingly competitive with sympatric nonsucculent plants. For example, *Mesembryanthemum crystallinum* (Aizoaceae) and *Cylindropuntia imbricate* (Cactaceae) begin to outcompete sympatric C_3 and C_4 grasses under drier conditions (Huang et al., 2020; Yu et al., 2019). In addition, succulent species have become invasive aliens in a number of ecosystems across the world (Herrando-Moraira et al., 2020; Novoa et al., 2014; Osmond et al., 2007). Field trials are underway to utilise this adaptive advantage by growing succulent *Agave* and *Opuntia* as bioenergy crops in marginal lands (Davis et al., 2017; Neupane et al., 2021). However, little has been done to

quantify to what extent CAM and C_{FT} are relatively responsible for any competitive advantage succulent plants experience under arid conditions. Having established that CAM and C_{FT} are independent traits in *Clusia* leaves, we investigated the roles that each trait plays during drought, by simulating Panamanian dry season conditions with the Photo3 model (Hartzell et al., 2018). Our model indicated that CAM was more effective than C_{FT} at mitigating plant water stress in *Clusia* (Figures 7 and 8). Over a 24 h period, CAM substantially minimised fluctuations in Ψ_L . This finding is congruent with recent work in South Africa's Succulent Karoo, which found that the CAM species *Malephora purpureo-crocea* (Aizoaceae) exhibited substantially dampened diel fluctuations to Ψ_L , compared to the sympatric succulent C_3 species, *Augea capensis* (Zygophyllaceae) (Veste & Herppich, 2021). Our model also showed that whilst elevated C_{FT} did reduce fluctuations in Ψ_L , this effect was considerably less than that of CAM. Moreover, the presence of CAM resulted in plants losing less water from transpiration. Consequently, Ψ_{min} stayed relatively constant for about 15 days longer into the dry season in the CAM simulations, compared with the simulation of C_3 plants (Figure 8). In addition, CAM had a dramatic benefit to A_n during drought. Despite the CAM plants assimilating less CO_2 than the C_3 plants under well-watered conditions, the ability to mitigate water loss prevented drops in Ψ_L and allowed stomata to stay open for longer into the dry season (Figure 8). Hence, by the end of the 50-day dry-down both CAM simulations had achieved 65% higher cumulative carbon uptake than either C_3 scenario. In contrast to CAM, C_{FT} had only a small impact on gas exchange and Ψ_L (Figure 8). Therefore, the benefits achieved from using CAM to prevent water loss appear to far outstrip those gained from using C_{FT} to buffer Ψ_L , in *Clusia*. Together, these results indicate that CAM is more beneficial to photosynthesis and water conservation than elevated C_{FT} , suggesting that this metabolic adaptation can drive the increased competitive advantage of succulent plants in nature.

In addition to comparing the contributions of different adaptations during drought, modelling can provide valuable insights into the ways in which physiological traits interact with different forms of photosynthesis (Iqbal et al., 2021). Our model found that C_{FT} had a substantially smaller effect on gas exchange rates and diel Ψ_L in the CAM background, in comparison to the C_3 simulations (Figures 7 and 8). This suggests that the presence of CAM largely obviates the effect of hydrenchyma-derived C_{FT} as an adaptation to drought. These predictions agree with the recent ecological finding that CAM, and not hydrenchyma thickness, correlates with environmental precipitation deficits across the ecological range of *Clusia* (Leverett et al., 2021). However, the outcome of this modelling brings into question why hydrenchyma thickness and C_{FT} vary so much across *Clusia* (Supporting Information: Figure S2). Why do species evolve deeper hydrenchyma tissue, if CAM is a more effective adaptation to drought? One hypothesis is that hydrenchyma functions more effectively as an adaptation to cloud cover at high altitudes. In high elevation tropical forests, clouds can often obscure the sun for large portions of the day (Pierce et al., 2002). Being able to buffer Ψ_L for short periods of direct sunlight in montane cloud forests would allow

leaves to maximise A_n when light is momentarily available, as stomata could stay open, despite water loss. An analogous phenomenon is known to occur in shade leaves; if stomata can stay open despite water loss, shade leaves will benefit from high gas exchange rates when a transitory sun fleck occurs (Schymanski et al., 2013). Hydrenchyma thickness is often high in species living in montane cloud forests (Earnshaw et al., 1987; Tanner & Kapos, 1982), and this trend held true in *Clusia*. In a pilot study of Panamanian *Clusia* species, we found that hydrenchyma thickness was higher in species living at high elevation compared to those sampled in the lowlands (Supporting Information: File). More work is required to explore the ecophysiological connection between hydrenchyma thickness and altitude in tropical trees. Nevertheless, it is clear that hydrenchyma, and the elevated C_{FT} this tissue provides, is a physiologically distinct adaptation, independent of CAM, in the genus *Clusia*.

5 | CONCLUSIONS

CAM is often found alongside tissue succulence, which has led many to speculate that this photosynthetic adaptation is always accompanied by elevated C_{FT} . In this study, we showed that CAM is independent of C_{FT} , in the genus *Clusia*. In addition, the anatomical adaptations accompanying CAM (large palisade chlorenchyma cells) do not confer additional C_{FT} , as this function is performed by the specialised hydrenchyma tissue. The lack of a relationship between chlorenchyma cell size and C_{FT} increases the likelihood that the former adaptation has evolved specifically to enable CAM, and not to serve any other purpose. Finally, modelling gas exchange and water relations during a Panamanian dry season predicted that CAM is substantially more beneficial than C_{FT} in increasing net carbon gain and buffering leaf water status during drought, in *Clusia*. This highlights the benefits of CAM and demonstrates the importance of understanding this photosynthetic adaptation in a hotter, drier world. Furthermore, our physiological framework for describing the relationship between leaf anatomy, CAM and C_{FT} sets a platform to explore the eco-evolutionary dynamics that have led to the emergence of different succulent phenotypes.

ACKNOWLEDGEMENT

The authors thank Samuel A. Logan and Helen Martin for assistance moving *Clusia* branches and plants. This research was partially funded by Newcastle University's R. B. Cook Scholarship and a Smithsonian Tropical Research Institute Short Term Fellowship to AL.

DATA AVAILABILITY STATEMENT

The data that support the findings of this study are available from the corresponding author upon reasonable request.

All data and R scripts are available upon request.

REFERENCES

Abraham, P.E., Hurtado Castano, N., Cowan-Turner, D., Barnes, J., Poudel, S., Hettich, R. et al. (2020) Peeling back the layers of

- crassulacean acid metabolism: functional differentiation between *Kalanchoë fedtschenkoi* epidermis and mesophyll proteomes. *The Plant Journal*, 103(2), 869–888. <https://doi.org/10.1111/tpj.14757>
- Ahl, L.I., Mravec, J., Jørgensen, B., Rudall, P.J., Rønsted, N. & Grace, O.M. (2019) Dynamics of intracellular mannan and cell wall folding in the drought responses of succulent *Aloe* species. *Plant, cell & environment*, 42, 2458–2471. <https://doi.org/10.1111/pce.13560>
- Arakaki, M., Christin, P.-A., Nyffeler, R., Lendel, A., Eggli, U. & Ogburn, R.M. et al. (2011) Contemporaneous and recent radiations of the world's major succulent plant lineages. *Proceedings of the National Academy of Sciences*, 108(20), 8379–8384. <https://doi.org/10.1073/pnas.1100628108>
- Arndt, S.K., Irawan, A. & Sanders, G.J. (2015) Apoplastic water fraction and rehydration techniques introduce significant errors in measurements of relative water content and osmotic potential in plant leaves. *Physiologia Plantarum*, 155(4), 355–368. <https://doi.org/10.1111/pp1.12380>
- Barrera-Zambrano, V.A., Lawson, T., Olmos, E., Fernandez-Garcia, N. & Borland, A.M. (2014) Leaf anatomical traits which accommodate the facultative engagement of crassulacean acid metabolism in tropical trees of the genus *Clusia*. *Journal of Experimental Botany*, 65(13), 3513–3523. <https://doi.org/10.1093/jxb/eru022>
- Bartlett, M.S., Vico, G. & Porporato, A. (2014) Coupled carbon and water fluxes in CAM photosynthesis: modeling quantification of water use efficiency and productivity. *Plant and Soil*, 383(1–2), 111–138. <https://doi.org/10.1007/s11104-014-2064-2>
- Beadle, C. L., Ludlow, M. M. & Honeysett, J. L. (1985) Water Relations. In: Coombs, J., Hall, D. O., Long, S. P. & Scurlock, J. M. O. (Eds.) *Techniques in Bioproductivity and Photosynthesis*, 2nd ed. Pergamon, pp. 50–61.
- Blackman, C.J. & Brodribb, T.J. (2011) Two measures of leaf capacitance: Insights into the water transport pathway and hydraulic conductance in leaves. *Functional Plant Biology*, 38(2), 118–126. <https://doi.org/10.1071/FP10183>
- Borland, A.M., Griffiths, H., Maxwell, C., Broadmeadow, M.S.J., Griffiths, N.M. & Barnes, J.D. (1992) On the ecophysiology of the Clusiaceae in Trinidad: expression of CAM in *Clusia minor* L. during the transition from wet to dry season and characterization of three endemic species. *New Phytologist*, 122(2), 349–357. <https://doi.org/10.1111/j.1469-8137.1992.tb04240.x>
- Borland, A. M., Leverett, A., Hurtado-Castano, N., Hu, R. & Yang, X. (2018) Functional Anatomical Traits of the Photosynthetic Organs of Plants with Crassulacean Acid Metabolism. In: Adams, W. W., III & Terashima, I. (Eds.) *The Leaf: A Platform for Performing Photosynthesis*, 1st ed., pp. 281–305. https://doi.org/10.1007/978-3-319-93594-2_10
- Borland, A.M., Wullschleger, S.D., Weston, D.J., Hartwell, J., Tuskan, G.a, Yang, X. et al. (2015) Climate-resilient agroforestry: physiological responses to climate change and engineering of crassulacean acid metabolism (CAM) as a mitigation strategy. *Plant, Cell & Environment*, 38, 1833–1849. <https://doi.org/10.1111/pce.12479>
- Braybrook, S.A., Hofte, H. & Peaucelle, A. (2012) Probing the mechanical contributions of the pectin matrix: Insights for cell growth. *Plant Signaling & Behavior*, 7(8), 1037–1041. <https://doi.org/10.4161/psb.20768>
- Brodribb, T.J., Skelton, R.P., Mcadam, S.A.M., Bienaimé, D., Lucani, C.J. & Marmottant, P. (2016) Visual quantification of embolism reveals leaf vulnerability to hydraulic failure. *New Phytologist*, 209(4), 1403–1409. <https://doi.org/10.1111/nph.13846>
- Chomthong, M. & Griffiths, H. (2020) Model approaches to advance crassulacean acid metabolism system integration. *The Plant Journal*, 101(4), 951–963. <https://doi.org/10.1111/tpj.14691>
- Davis, S.C., Kuzmick, E.R., Niechayev, N. & Hunsaker, D.J. (2017) Productivity and water use efficiency of *Agave americana* in the first field trial as bioenergy feedstock on arid lands. *GCB Bioenergy*, 9(2), 314–325. <https://doi.org/10.1111/gcbb.12324>
- Earnshaw, M.J., Winter, K., Ziegler, H., Stichler, W., Cruttwell, N.E.G., Kerenga, K. et al. (1987) Altitudinal changes in the incidence of crassulacean acid metabolism in vascular epiphytes and related life forms in Papua New Guinea. *Oecologia*, 73, 566–572.
- Edwards, E.J. (2019) Evolutionary trajectories, accessibility, and other metaphors: the case of C_4 and CAM photosynthesis. *New Phytologist*, 223(4), 1742–1755. <https://doi.org/10.1111/nph.15851>
- Fradera-Soler, M., Grace, O.M., Jørgensen, B. & Mravec, J. (2022) Elastic and collapsible: current understanding of cell walls in succulent plants. *Journal of Experimental Botany*, 73(8), 2290–2307. <https://doi.org/10.1093/jxb/erac054>
- Fradera-Soler, M., Leverett, A., Mravec, J., Jørgensen, B., Borland, A.M. & Grace, O.M. (2022) Are cell wall traits a component of the succulent syndrome? *Frontiers in Plant Science*, 13, 1–10. <https://doi.org/10.3389/fpls.2022.1043429>
- Fradera-Soler, M., Rudall, P.J., Prychid, C.J. & Grace, O.M. (2021) Evolutionary success in arid habitats: Morpho-anatomy of succulent leaves of *Crassula* species from southern Africa. *Journal of Arid Environments*, 185(February), 104319. <https://doi.org/10.1016/j.jaridenv.2020.104319>
- Germon, A., Jourdan, C., Bordron, B., Robin, A., Nouvellon, Y., Chapuis-Lardy, L. et al. (2019) Consequences of clear-cutting and drought on fine root dynamics down to 17 m in coppice-managed eucalypt plantations. *Forest Ecology and Management*, 445, 48–59. <https://doi.org/10.1016/j.foreco.2019.05.010>
- Goycoolea, F.M. & Cárdenas, A. (2003) Pectins from *Opuntia* spp.: A short review. *Journal of the Professional Association for Cactus Development*, 5(May), 17–29.
- Hartzell, S., Bartlett, M.S., Inglese, P., Consoli, S., Yin, J. & Porporato, A. (2021) Modelling nonlinear dynamics of Crassulacean acid metabolism productivity and water use for global predictions. *Plant, Cell & Environment*, 44(1), 34–48. <https://doi.org/10.1111/pce.13918>
- Hartzell, S., Bartlett, M.S. & Porporato, A. (2018) Unified representation of the C_3 , C_4 , and CAM photosynthetic pathways with the Photo3 model. *Ecological Modelling*, 384(June), 173–187. <https://doi.org/10.1016/j.ecolmodel.2018.06.012>
- Hartzell, S., Bartlett, M.S., Virgin, L. & Porporato, A. (2015) Nonlinear dynamics of the CAM circadian rhythm in response to environmental forcing. *Journal of Theoretical Biology*, 368, 83–94. <https://doi.org/10.1016/j.jtbi.2014.12.010>
- Herrando-Mora, S., Vitales, D., Nualart, N., Gómez-Bellver, C., Ibáñez, N., Massó, S. et al. (2020) Global distribution patterns and niche modelling of the invasive *Kalanchoe × houghtonii* (Crassulaceae). *Scientific Reports*, 10(1), 3143. <https://doi.org/10.1038/s41598-020-60079-2>
- Heyduk, K. (2021) The genetic control of succulent leaf development. *Current Opinion in Plant Biology*, 59, 101978. <https://doi.org/10.1016/j.pbi.2020.11.003>
- Heyduk, K., Burrell, N., Lalani, F. & Leebens-Mack, J. (2016) Gas exchange and leaf anatomy of a C_3 -CAM hybrid, *Yucca gloriosa* (Asparagaceae). *Journal of Experimental Botany*, 67(5), 1369–1379. <https://doi.org/10.1093/jxb/erv536>
- Heyduk, K., Grace, O.M. & McKain, M.R. (2021) Life Without Water. *American Journal of Botany*, 108(2), 181–183. <https://doi.org/10.1002/ajb2.1615>
- Holtum, J.A.M., Aranda, J., Virgo, A., Gehrig, H.H. & Winter, K. (2004) $\delta^{13}C$ values and crassulacean acid metabolism in *Clusia* species from Panama. *Trees*, 18, 658–668. <https://doi.org/10.1007/s00468-004-0342-y>
- Huang, H., Yu, K. & D'Odorico, P. (2020) CAM plant expansion favored indirectly by asymmetric climate warming and increased rainfall variability. *Oecologia*, 193(1), 1–13. <https://doi.org/10.1007/s00442-020-04624-w>
- Iqbal, W.A., Miller, I.G., Moore, R.L., Hope, I.J., Cowan-Turner, D. & Kapralov, M.V. (2021) Rubisco substitutions predicted to enhance

- crop performance through carbon uptake modelling. *Journal of Experimental Botany*, 72(17), 6066–6075.
- Jiao, W., Wang, L., Smith, W.K., Chang, Q., Wang, H. & D'Odorico, P. (2021) Observed increasing water constraint on vegetation growth over the last three decades. *Nature Communications*, 12(1), 3777. <https://doi.org/10.1038/s41467-021-24016-9>
- John, G.P., Henry, C. & Sack, L. (2018) Leaf rehydration capacity: Associations with other indices of drought tolerance and environment. *Plant, Cell & Environment*, 41(11), 2638–2653. <https://doi.org/10.1111/pce.13390>
- Jolly, A.R., Zailaa, J., Farah, U., Woojuh, J., Libifani, F.M., Arzate, D. et al. (2020) Leaf Venation and Morphology Help Explain Physiological Variation in *Yucca brevifolia* and *Hesperoyucca whipplei* Across Microhabitats in the Mojave Desert, CA. *Frontiers in Plant Science*, 11(January), 578338. <https://doi.org/10.3389/fpls.2020.578338>
- Kim, S.J., Chandrasekar, B., Rea, A.C., Danhof, L., Zemelis-Durfee, S. & Thrower, N. (2020) The synthesis of xyloglucan, an abundant plant cell wall polysaccharide, requires CSLC function. *Proceedings of the National Academy of Sciences of the United States of America*, 117(33), 20316–20324. <https://doi.org/10.1073/PNAS.2007245117>
- Leverett, A., Ferguson, K., Winter, K. & Borland, A.M. (2022) Exploring xylem anatomical adaptations associated with crassulacean acid metabolism and hydraulic capacitance in *Clusia* leaves: lessons for CAM Bioengineering. *BioRxiv*. <https://doi.org/10.1101/2022.05.27.493620>
- Leverett, A., Hurtado Castaño, N., Ferguson, K., Winter, K. & Borland, A.M. (2021) Crassulacean acid metabolism (CAM) supercedes the turgor loss point (TLP) as an important adaptation across a precipitation gradient, in the genus *Clusia*. *Functional Plant Biology*, 48(7), 703–716. <https://doi.org/10.1071/FP20268>
- Luján, M., Oleas, N.H. & Winter, K. (2021) Evolutionary history of CAM photosynthesis in Neotropical *Clusia*: insights from genomics, anatomy, physiology and climate. *Botanical Journal of the Linnean Society*, 199(2), 538–536. <https://doi.org/10.1093/botlinnean/boab075>
- Luo, Y., Ho, C.-L., Helliker, B.R. & Katifori, E. (2021) Leaf Water Storage and Robustness to Intermittent Drought: A Spatially Explicit Capacitive Model for Leaf Hydraulics. *Frontiers in Plant Science*, 12(October), 725995. <https://doi.org/10.3389/fpls.2021.725995>
- Males, J. (2017) Secrets of succulence. *Journal of Experimental Botany*, 68(9), 2121–2134. <https://doi.org/10.1093/jxb/erx096>
- Males, J. (2018) Concerted anatomical change associated with crassulacean acid metabolism in the Bromeliaceae. *Functional Plant Biology*, 45(7), 681–695. <https://doi.org/10.1071/fp17071>
- Males, J. & Griffiths, H. (2018) Economic and hydraulic divergences underpin ecological differentiation in the Bromeliaceae. *Plant, Cell & Environment*, 41(1), 64–78. <https://doi.org/10.1111/pce.12954>
- Martin, C.E., Herppich, W.B., Roscher, Y. & Burkart, M. (2019) Relationships between leaf succulence and Crassulacean acid metabolism in the genus *Sansevieria* (Asparagaceae). *Flora*, 261(April), 151489. <https://doi.org/10.1016/j.flora.2019.151489>
- Mauseth, J.D. (1995) Collapsible Water-Storage Cells in Cacti. *Bulletin of the Torrey Botanical Club*, 122(2), 145–151.
- Maxwell, K., Von Caemmerer, S. & Evans, J.R. (1997) Is a low internal conductance to CO₂ diffusion a consequence of succulence in plants with crassulacean acid metabolism. *Australian Journal of Plant Physiology*, 24(6), 777–786. <https://doi.org/10.1071/PP97088>
- Mcadam, S.A.M. & Brodribb, T.J. (2013) Ancestral stomatal control results in a canalization of fern and lycophyte adaptation to drought. *New Phytologist*, 198(2), 429–441. <https://doi.org/10.1111/nph.12190>
- Merklinger, F.F., Böhner, T., Arakaki, M., Weigend, M., Quandt, D. & Luebert, F. (2021) Quaternary diversification of a columnar cactus in the driest place on earth. *American Journal of Botany*, 108(2), 184–199. <https://doi.org/10.1002/ajb2.1608>
- Messerschmid, T.F.E., Wehling, J., Bobon, N., Kahmen, A., Klak, C., Los, J.A. et al. (2021) Carbon isotope composition of plant photosynthetic tissues reflects a Crassulacean Acid Metabolism (CAM) continuum in the majority of CAM lineages. *Perspectives in Plant Ecology, Evolution and Systematics*, 51(June), 125619. <https://doi.org/10.1016/j.ppees.2021.125619>
- Moller, I., Sørensen, I., Bernal, A.J., Blaukopf, C., Lee, K., Øbro, J. et al. (2007) High-throughput mapping of cell-wall polymers within and between plants using novel microarrays. *The Plant Journal*, 50(6), 1118–1128. <https://doi.org/10.1111/j.1365-3113X.2007.03114.x>
- Nelson, E.a, Sage, T.L. & Sage, R.F. (2005) Functional leaf anatomy of plants with crassulacean acid metabolism. *Functional Plant Biology*, 32(5), 409–419. <https://doi.org/10.1071/FP04195>
- Neupane, D., Mayer, J.A., Niechayev, N.A., Bishop, C.D. & Cushman, J.C. (2021) Five-year field trial of the biomass productivity and water input response of cactus pear (*Opuntia* spp.) as a bioenergy feedstock for arid lands. *GCB Bioenergy*, 13(4), 719–741. <https://doi.org/10.1111/gcbb.12805>
- Novoa, A., Le Roux, J.J., Robertson, M.P., Wilson, J.R. & Richardson, D.M. (2014) Introduced and invasive cactus species: a global review. *AoB Plants*, 7(1), 1–14. <https://doi.org/10.1093/aobpla/plu078>
- Nowak, E.J. & Martin, C.E. (1997) Physiological and Anatomical Responses to Water Deficits in the CAM Epiphyte *Tillandsia ionantha* (Bromeliaceae). *International Journal of Plant Sciences*, 158(6), 818–826.
- Ogburn, R.M. & Edwards, E.J. (2012) Quantifying succulence: A rapid, physiologically meaningful metric of plant water storage. *Plant, Cell & Environment*, 35(9), 1533–1542. <https://doi.org/10.1111/j.1365-3040.2012.02503.x>
- Ogburn, R. M. & Edwards, E. J. (2010) The ecological water-use strategies of succulent plants. In: Kader, J.-C. & Delseny, M. (Eds.) *Advances in Botanical Research*, 1st ed. 55. Elsevier Ltd, pp. 179–225. <https://doi.org/10.1016/B978-0-12-380868-4.00004-1>
- Ong, B.-L., Koh, C.K.-K. & Wee, Y.-C. (1992) Changes in Cell Wall Structure of *Pyrrosia piloselloides* (L.) Price Leaf Cells During Water Stress. *International Journal of Plant Sciences*, 153(3), 329–332.
- Osmond, B., Neales, T. & Stange, G. (2007) Curiosity and context revisited: Crassulacean acid metabolism in the Anthropocene. *Journal of Experimental Botany*, 59(7), 1489–1502. <https://doi.org/10.1093/jxb/ern052>
- Pachon, P., Winter, K. & Lasso, E. (2022) Updating the occurrence of crassulacean acid metabolism (CAM) in the genus *Clusia* through carbon isotope analysis of species from Colombia. *Photosynthetica*, 60(2), 304–322. <https://doi.org/10.32615/ps.2022.018>
- Panter, P.E., Panter, J.R. & Knight, H. (2020) Impact of cell-wall structure and composition on plant freezing tolerance. *Annual Plant Reviews Online*, 3(4), 607–642. <https://doi.org/10.1002/9781119312994.apr0746>
- Pierce, S., Winter, K. & Griffiths, H. (2002) The role of CAM in high rainfall cloud forests: an in situ comparison of photosynthetic pathways in Bromeliaceae. *Plant, Cell and Environment*, 25, pp. 1181–1189. <https://doi.org/10.1046/j.1365-3040.2002.00900.x/pdf>
- Sáenz, C., Sepúlveda, E. & Matsuhira, B. (2004) *Opuntia* spp. mucilage's: A functional component with industrial perspectives. *Journal of Arid Environments*, 57(3), 275–290. [https://doi.org/10.1016/S0140-1963\(03\)00106-X](https://doi.org/10.1016/S0140-1963(03)00106-X)
- Schulte, P.J. & Nobel, P.S. (1989) Responses of a CAM Plant to Drought and Rainfall: capacitance and Osmotic Pressure Influences on Water Movement. *Journal of Experimental Botany*, 40(210), 61–70. <https://doi.org/10.1093/jxb/40.1.61%0Apapers2://publication//10.1093/jxb/40.1.61>
- Schymanski, S.J., Or, D. & Zwieniecki, M. (2013) Stomatal Control and Leaf Thermal and Hydraulic Capacitances under Rapid Environmental Fluctuations. *PLoS One*, 8(1), e54231. <https://doi.org/10.1371/journal.pone.0054231>

- Scoffoni, C., Albuquerque, C., Brodersen, C.R., Townes, S.V., John, G.P., Bartlett, M.K. et al. (2017) Outside-Xylem Vulnerability, Not Xylem Embolism, Controls Leaf Hydraulic Decline during Dehydration. *Plant Physiology*, 173(2), 1197–1210. <https://doi.org/10.1104/pp.16.01643>
- Scoffoni, C., Chatelet, D.S., Pasquet-Kok, J., Rawls, M., Donoghue, M.J., Edwards, E.J. et al. (2016) Hydraulic basis for the evolution of photosynthetic productivity. *Nature Plants*, 2(6), 16072. <https://doi.org/10.1038/nplants.2016.72>
- Sheffield, J. & Wood, E.F. (2008) Global trends and variability in soil moisture and drought characteristics, 1950–2000, from observation-driven simulations of the terrestrial hydrologic cycle. *Journal of Climate*, 21(3), 432–458. <https://doi.org/10.1175/2007JCLI1822.1>
- Smith, J.A.C., Schulte, P.J. & Nobel, P.S. (1987) Water flow and water storage in *Agave deserti*: osmotic implications of crassulacean acid metabolism. *Plant, Cell & Environment*, 10, 639–648.
- Tanner, E.V.J. & Kapos, V. (1982) Leaf Structure of Jamaican Upper Montane Rain-Forest Trees. *Biotropica*, 14(1), 16–24.
- Tay, I., Odang, K.B. & Cheung, C. (2020) Metabolic Modeling of the C₃-CAM Continuum Revealed the Establishment of a Starch/Sugar-Malate Cycle in CAM Evolution. *Frontiers in Plant Science*, 11(January), 573197. <https://doi.org/10.3389/fpls.2020.573197>
- Tinoco Ojanguren, C. & Vázquez Yanes, C. (1983) Especies CAM en la selva húmeda tropical de los tuxtlas, Veracruz. *Boletín de La Sociedad Botánica de México*, 45(March 1983), 150–153.
- Töpfer, N., Braam, T., Shameer, S., Ratcliffe, R.G. & Sweetlove, L.J. (2020) Alternative crassulacean acid metabolism modes provide environment-specific water-saving benefits in a leaf metabolic model. *The Plant Cell*, 32(12), 3689–3705. <https://doi.org/10.1105/tpc.20.00132>
- Trueba, S., Pan, R., Scoffoni, C., John, G.P., Davis, S.D. & Sack, L. (2019) Thresholds for leaf damage due to dehydration: declines of hydraulic function, stomatal conductance and cellular integrity precede those for photochemistry. *New Phytologist*, 223(1), 134–149. <https://doi.org/10.1111/nph.15779>
- Vanzin, G.F., Madson, M., Carpita, N.C., Raikhel, N.V., Keegstra, K. & Reiter, W.D. (2002) The *mur2* mutant of *Arabidopsis thaliana* lacks fucosylated xyloglucan because of a lesion in fucosyltransferase AtFUT1. *Proceedings of the National Academy of Sciences*, 99(5), 3340–3345. <https://doi.org/10.1073/pnas.052450699>
- Veste, M. & Herppich, W.B. (2021) Comparative ecophysiology of the leaf-succulents *Augea capensis* (C₃) and *Malephora purpureo-crocea* (CAM) in the Knersvlakte, Succulent Karoo, South Africa. *Flora*, 278(August 2020), 151807. <https://doi.org/10.1016/j.flora.2021.151807>
- Winter, K. (2019) Ecophysiology of constitutive and facultative CAM photosynthesis. *Journal of Experimental Botany*, 70(22), 6495–6508. <https://doi.org/10.1093/jxb/erz002>
- Winter, K., Aranda, J. & Holtum, J.A.M. (2005) Carbon isotope composition and water-use efficiency in plants with crassulacean acid metabolism. *Functional Plant Biology*, 32(5), 381–388. <https://doi.org/10.1071/FP04123>
- Winter, K. & Holtum, J.A.M. (2014) Facultative crassulacean acid metabolism (CAM) plants: powerful tools for unravelling the functional elements of CAM photosynthesis. *Journal of Experimental Botany*, 65(13), 3425–3441. <https://doi.org/10.1093/jxb/eru063>
- Yamaga-Hatakeyama, Y., Okutani, M., Hatakeyama, Y., Yabiku, T., Yukawa, T. & Ueno, O. (2022) Photosynthesis and leaf structure of F₁ hybrids between *Cymbidium ensifolium* (C₃) and *C. bicolor* subsp. *pubescens* (CAM). *Annals of Botany*. <https://doi.org/10.1093/aob/mcac157/6964910>
- Yang, X., Cushman, J.C., Borland, A.M. & Liu, Q. (2020) Editorial: Systems Biology and Synthetic Biology in Relation to Drought Tolerance or Avoidance in Plants. *Frontiers in Plant Science*, 11(April), 2018–2021. <https://doi.org/10.3389/fpls.2020.00394>
- Yu, K., D'Odorico, P., Collins, S.L., Carr, D., Porporato, A., Anderegg, W.R.L. et al. (2019) The competitive advantage of a constitutive CAM species over a C₄ grass species under drought and CO₂ enrichment. *Ecosphere*, 10(5), e02721. <https://doi.org/10.1002/ecs2.2721>
- Zhang, Y.-J., Rockwell, F.E., Graham, A.C., Alexander, T. & Holbrook, N.M. (2016) Reversible Leaf Xylem Collapse: A Potential “Circuit Breaker” against Cavitation. *Plant Physiology*, 172(4), 2261–2274. <https://doi.org/10.1104/pp.16.01191>

SUPPORTING INFORMATION

Additional supporting information can be found online in the Supporting Information section at the end of this article.

How to cite this article: Leverett, A., Hartzell, S., Winter, K., Garcia, M., Aranda, J., Virgo, A., et al. (2023) Dissecting succulence: Crassulacean acid metabolism and hydraulic capacitance are independent adaptations in *Clusia* leaves. *Plant, Cell & Environment*, 1–17. <https://doi.org/10.1111/pce.14539>